RSC Advances

PAPER

View Article Online
View Journal | View Issue

Cite this: *RSC Adv.*, 2022, **12**, 3216

Mechanism unravelling for highly efficient and selective $^{99}TcO_4^-$ sequestration utilising crown ether based solvent system from nuclear liquid waste: experimental and computational investigations

Kankan Patra,*[a] Arijit Sengupta,*[bc] Anil Boda,[d] Musharaf Ali,[d] V. K. Mittal,[a] T. P. Valsala[a] and C. P. Kaushik[ce]

Selective and efficient separation of pertechnetate (TcO_4^-) from nuclear waste is desirable for the safe and secure management of radioactive waste. Here, we have projected dibenzo-18-crown-6 ether (DB18C6) in a highly polar nitrobenzene medium for enhancing the removal efficiency of ^{99}Tc from reprocessing plant low level waste (LLW). An effort was made to determine the stoichiometry of metal–ligand complex by slope ratio method, revealing that one ligand (DB18C6) binds with one TcO_4^- moiety. Optimum ligand concentration for ^{99}Tc extraction was evaluated. Relevant interference of the anions was studied systematically. The effect of solution pH was analysed on the extraction efficiency of ^{99}Tc. A kinetic study was carried out for maximum extraction of metal ions. A quantitative stripping study was also achieved for metal ions with a suitable stripping solution. After evaluation of all essential parameters, selectivity and feasibility studies were finally carried out with actual low level reprocessing plant waste to demonstrate a laboratory scale process for effective separation of TcO_4^- ions. Density functional theory (DFT) calculations were carried out to understand the nature of the complexation of TcO_4^- ion with DB18C6 in different solvents systems and to elucidate the key aspect behind ionic selectivity and enhanced the ^{99}Tc extraction efficiency of DB18C6 in the studied diluent systems. The ΔE and ΔG values for different modeled complexation reactions were evaluated systematically. From the calculated free energy of complexation of TcO_4^- with DB18C6, it was observed that the consideration of explicit solvent plays a vital role in predicting the experimental selectivity.

Received 20th October 2021
Accepted 3rd January 2022

DOI: 10.1039/d1ra07738d

rsc.li/rsc-advances

1. Introduction

Presently, nuclear power is a growing technology that can fulfill the high demand for low-carbon energy globally.[1–6] The progress of nuclear industries has been associated with some issues such as accidental and intentional release of harmful radionuclides in the environment.[7,8] The success and public acceptance of nuclear industries depend on the safe and secure management of hazardous radioactive waste. Out of several radionuclides, one potentially troublesome radionuclide is ^{99}Tc, a beta emitting radionuclide ($E_{\beta\text{-max}} = 295.5$ keV) having long half-life ($t_{1/2} = 2.13 \times 10^5$ y),[9] ^{99}Tc is generated during the fission of ^{235}U with a 6.13% yield.[10] ^{99}Tc is mostly found as TcO_4^- species in the aqueous system, where it exists in a +7 oxidation state. Unlike MnO_4^- ions, $^{99}TcO_4^-$ does not have a strong oxidizing capacity, making it extremely stable under different environmental conditions. Additionally, $^{99}TcO_4^-$ moiety possesses high symmetric geometrical configuration (T_d) and low charge density, making it quite non-complexing in nature, along with high solubility (11.3 M at 20 °C).[11–14]

Consequently, $^{99}TcO_4^-$ can easily migrate into the environment through a natural water system, and at the same time, it is difficult to capture by using a majority of conventional materials, thereby posing severe environmental risks.

Due to the volatile nature of ^{99}Tc compounds (*e.g.*, Tc_2O_7), vitrification of nuclear waste at high temperatures gets affected, and it creates challenges in the off-gas system design for waste management facilities.[15] ^{99}Tc vapor inhalation and dust contamination can create a major cancer risk,[16] while after digestion, ^{99}Tc can build up in the thyroid and mammary tissue.[17] Considering all these factors, separation of ^{99}Tc is an

[a]*Nuclear Recycle Board, Bhabha Atomic Research Centre, Tarapur, 401504, India. E-mail: kankan.patra2010@gmail.com*

[b]*Radiochemistry Division, Bhabha Atomic Research Centre, Mumbai 400 085, India. E-mail: arijitbarc@gmail.com*

[c]*Homi Bhabha National Institute, Anushaktinagar, Mumbai 400 094, India*

[d]*Chemical Engineering Division, Bhabha Atomic Research Centre, Mumbai 400 085, India*

[e]*Nuclear Recycle Group, Bhabha Atomic Research Centre, Mumbai 400 085, India*

urgent need to ensure safe and secured management of highly toxic radioactive waste as well as to reduce ^{99}Tc release through off-site migration to contaminate groundwater.[15] Therefore, efficient and selective separation of radioactive ^{99}Tc has drawn significant attention in the nuclear industry.

Due to reprocessing of spent nuclear fuel, high level liquid waste (HLLW) and intermediate level liquid waste (ILLW) are generated in the reprocessing plant. ILLW is made alkaline with the addition of sodium hydroxide and sodium carbonate to store in carbon steel waste tank farms. Treatment of alkaline ILW is carried out *via* resorcinol formaldehyde (RF) resin and imino diacetic acid resin using ion exchange method to separate ^{137}Cs and ^{90}Sr, respectively. After separation of ^{137}Cs and ^{90}Sr from ILLW, it reduces its activity and gets converted to low level waste (LLW), which contains mainly ^{99}Tc and ^{106}Ru. It is very much essential to separate ^{99}Tc and ^{106}Ru before discharge, mainly to bring down the activity level below the discharge limit.[18,19] As LLW contains high concentrations of monoanions like OH^- and NO_3^-, it is very challenging to separate TcO_4^- from alkaline waste due to the common ion effect. Preferably, TcO_4^- should be separated at the beginning stage while the spent nuclear fuel is chopped, followed by dissolution in concentrated nitric acid even before the PUREX (plutonium uranium redox extraction) process in the reprocessing plant. However, this early stage TcO_4^- separation is associated with a huge challenge given the extreme conditions prevailing like high ionic strength, super acidity as well as strong ionizing radiation.

Remarkable efforts have been given for designing efficient anion-exchange materials for the separation of TcO_4^- ions.[15] Conventional polymeric anion-exchange resins revealed efficient separation of TcO_4^- under acidic conditions,[20–22] but it is not radiation resistant. The kinetics of anion-exchange is usually quite slow, resulting in prolonged exposure of resins under radiation dose causing damage to the material due to the radiation effect. In this regard, some promising materials have been reported, like layered rare-earth hydroxides (LRHs),[23] layered double hydroxides (LDHs),[24,25] and thorium borates (NDTB-1).[26,27] These materials can work efficiently under radiation, but finally, these materials are not applicable in real time due to their poor selectivity as well as low sorption efficiency. In recent times, other potential candidates, known as cationic metal–organic frameworks (MOFs), have been reported for the separation of TcO_4^- from aqueous solution.[28–31] They exhibit fast sorption kinetics, excellent selectivity, high capacity, and great radiation resistance. However, these materials are not stable in highly acidic solutions, and these materials can show their effectiveness for environmental remediation under neutral conditions, but in the cases of reprocessing processes, these materials are not suitable.

For the removal of pertechnetate, some potential reagents like pyridines, SuperLig®639 resin, cyclohexanone, polyethylene glycols, tetraalkyl ammonium halides, tetraphenyl arsonium chloride (TPAC), *etc.* have been reported in the literature. Although they have shown promising results for the removal of TcO_4^- from waste, their real time applications for actual nuclear waste are limited to date.[32–37] For the removal of TcO_4^- ions from nuclear waste solution, various crown ethers have been explored. One of the promising candidates for the same is the di-*tert*-butylcyclohexano-18-crown-6 (di-*t*-BuCH18C6), which is dissolved in a mixture of Isobar® M and tributyl phosphate (TBP).[38] Very recently, Sharma *et al.*[39] optimized the composition of the diluent system for the organic phase based on dodecane and iso-decyl alcohol to efficiently extract ^{99}Tc using 0.2 M di-*t*-BuCH18C6 with D_{Tc} value of ~4.46. Crown ethers have major advantages with respect to any other conventional reagents for the removal of TcO_4^- ions as they can work in the presence of high salt concentrations. Hence, crown ethers can directly bind TcO_4^- ions without any pre-treatment of waste solutions containing high nitrate ions. In the case of crown ethers, the loaded solvent can be easily stripped with only water. Extraction of TcO_4^- ions by crown ethers occurs through ion pair formation, where crown ether forms complex with monocations (mainly sodium), like crown ether-sodium metal ion complexes, and TcO_4^- ions neutralize the charge of the complexes as counter ions. Complex formation of crown ethers with TcO_4^- is superior to OH^- and NO_3^- ions. This can be explained in terms of lower ionic hydration enthalpy of TcO_4^- ions (-251 kJ mol^{-1}) as compared to OH^- (-410 kJ mol^{-1}) and NO_3^- (-289 kJ mol^{-1}) ions, respectively.[40] The extraction efficiency is strongly controlled by complex formation and its stability.[39] Through computational studies, it has been confirmed that DB18C6 shows a strong binding affinity towards sodium ions in the solution phase.[41] Based on these understandings, we have selected a crown-ether, namely dibenzo-18-crown-6 (DB18C6), which is easily available in large scale, commercially cheap, and good in the extraction of sodium ions, and we have studied its extracting properties for TcO_4^- ions. Note that dibenzo-18-crown-6 is reasonably simple to synthesize with reproducible product quality.

In the extraction process, solvent polarities often play an important role. Thus, the dielectric constants of the used diluents have a direct influence over the extraction efficiency of metal ions. Accordingly, in addition to the selection of an appropriate ligand, the choice of a proper diluent is also an essential parameter to achieve enhanced efficiency of the extraction process. Keeping this in mind, here we have attempted to achieve an enhanced distribution ratio for TcO_4^- ions using well known ligand DB18C6 in a highly polar nitrobenzene medium, considering that metal extraction efficiency increases with the increased polarity of the organic solvent system.[42] Effects of solution pH and interferences of relevant anions on the extraction process of TcO_4^- ions have been systematically investigated. The optimum contact time for maximum extraction of TcO_4^- ions was estimated. Stripping studies were carried out using water and HNO_3. The DFT calculation was carried out to understand the complexation of TcO_4^- ion with DB18C6 in different solvents. The ΔE and ΔG values for different modelled complexation reactions were evaluated. From the calculated free energy of complexation of TcO_4^- with DB18C6, it was observed that the consideration of explicit solvent plays a very important role in predicting the experimental selectivity. Finally, after evaluation of all essential parameters for the optimum solvent system, we have effectively

demonstrated the feasibility study with an actual reprocessing waste solution to establish a process for TcO_4^- ion separation from alkaline LLW.

2. Experimental

2.1 Materials: chemicals, isotopes, and solutions

Nitrobenzene (NB) (99.9%) and DB18C6 (Fig. 1) were used as received (S.D. Fine). Each experiment was conducted in triplicate to confirm the reproducibility of the observations. ^{99}Tc radioisotope was separated from plant LLW by Sonar *et al.*,[43] which was used in the present investigation as a radiotracer. Compositions of LLW samples represented in Table 1 were generated from our reprocessing plant. Before reprocessing, the spent fuel from the pressurized heavy water reactor (burn up of 6500 MWD tone^{-1}) was cooled for 3 years and used subsequently for extraction studies in batch mode. During the experiment, proper personal protective equipment (PPE) and personal radiation monitoring instruments were used. We kept the solution activity less than 1 mCi L^{-1}, and also, the gamma radiation field was less than 1 mR h^{-1}. Supra-pure HNO_3 and quartz double distilled water were used throughout the present investigation.

2.2 Percent extraction, distribution studies, and radiometry

The extent of ^{99}Tc removal from the aqueous phase was determined by calculating the distribution ratio (D_{Tc}) or percent extraction (PE). All the studies were performed at (25 ± 1) °C, maintained using a thermostated water bath. The distribution ratio D_{Tc} for ^{99}Tc or D_M for any other metal can be calculated by estimating the ratio of the radioactivity/concentration in the organic phase to the radioactivity/concentration in the aqueous phase at equilibrium. Following the method adopted by Sonar *et al.*, the concentration of pertechnetate ion in an aqueous medium was calculated using the Tc – tetraphenyl arsonium chloride (TPAC) complex method.[43] Analysis of ^{99}Tc radionuclide was carried out by precipitating with TPAC complex followed by beta activity counting by GM counter to estimate the ^{99}Tc concentration in waste streams. During beta activity counting, self absorption of low energy beta particles through the precipitate introduces error. The concentration of ^{99}Tc was confirmed using its cgross beta cut-off (95%) by evaporation onto a planchet and Al-absorber having thickness 100 mg cm^{-2}.[43] Solution pH was measured using Benchtop pH meters. ZnS/Ag scintillator, GM counter, and NaI/Tl scintillator were used for the estimation of gross α, β and γ activities. To determine PE, the organic phase (DB18C6 in 100% nitrobenzene) and aqueous phase (pH 13, containing ^{99}Tc) were equilibrated in a 1 : 1 ratio for 20 min in a glass vial and centrifuged subsequently to separate the two phases. The error/uncertainty of the experimental result was within ±5%. The percentage of ^{99}Tc extraction was calculated using the following equation:

$$\text{Extraction\%} = \frac{\text{Tc activity in organic}}{\text{Tc activity in initial}} \times 100 \quad (1)$$

where Tc activity in organic = ^{99}Tc extracted from the organic phase, Tc activity in initial = total ^{99}Tc taken for extraction in the aqueous phase.

Table 1 Compositions of the LLW samples used in the present study

Species	Activity/concentration
Gross β	(0.40–0.50) mCi L^{-1}
Gross α	5 × 10^{-4} mCi L^{-1}
Gross γ	(8 × 10^{-3} to 6 × 10^{-2}) mCi L^{-1}
Sr-90	10^{-4} mCi L^{-1}
Cs-137	10^{-3} mCi L^{-1}
Ru-106	10^{-2} mCi L^{-1}
Sb-125	10^{-2} mCi L^{-1}
Tc-99	(0.1–0.3) mCi L^{-1}
Na^+	(1.3–1.8) M
NO_3^-	(2–3.5) M
pH	(11–13)

2.3 Computational protocol

The structure of DB18C6 and its complexes with TcO_4^- and Na^+ ions were optimized using B3LYP[44,45] functional with triple zeta valence plus polarization (TZVP) basis set as implemented in the Turbomole package.[46] The frequency calculations were carried at the same level, which is used for geometry optimization. The gas phase free energy, ΔG_g was computed at T = 298.15 K and P = 1 atm. The solvent effects were considered using the Conductor like Screening Model (COSMO)[47,48] solvation model. The default COSMO radii were used for all the elements. In the present study, we have considered three solvents, nitrobenzene, chlorobenzene, and trichloroethylene, to understand the experimental observations. Despite a lower dielectric constant, trichloroethylene has strong complexation compared to chlorobenzene, and nitrobenzene has a stronger complexation ability compared to the other two studied solvents because of its high dielectric constant. The dielectric constant, ε of water, nitrobenzene, chlorobenzene, and trichloroethylene, was taken as 80, 34.82, 5.62, and 3.42, respectively. The gas phase minimum energy structures were used for the calculation of single point energy in the COSMO phase.[49–54]

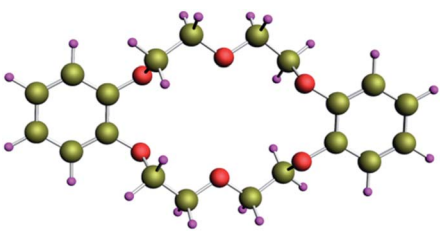

Fig. 1 Optimized structure of DB18C6.

3. Results and discussion

3.1 Kinetics study of ^{99}Tc extraction

Before starting the extraction studies, it is very important to evaluate the equilibrium time for maximum extraction of TcO_4^- ions. Keeping this in mind, the extraction profile for TcO_4^- was

established by varying the equilibration time. It was observed that at the time of about 15 min (Fig. 2), the reaction reached equilibrium, and subsequently, the D_{Tc} value was found to be almost unchanged. Hence, for all the extraction studies throughout the experiments, the equilibrium time was kept as 20 min.

As discussed earlier, LLW contained 1.3–1.8 M Na^+ in the form of nitrate. Therefore, the extraction kinetics shown above pertained to the mass transfer of Tc after the formation of the complex associated with Na^+ as well as BD18C6. It meant, while discussing the kinetics, it was not only the attachment of TcO_4^- to BD18C6, but it was the overall mass transfer of Tc after suitable complexation with ligand as well as Na^+ forming $[Na^+ \cdot BD18C6 \cdot TcO_4^-]_n$ like species.

3.2 Determination of metal–ligand binding stoichiometry

To determine the optimum ligand concentration for extraction of ^{99}Tc as well as to understand the complexation nature between the metal and ligand, an extraction study was carried out by varying the concentration of the DB18C6 ligand in the nitrobenzene solvent system (Fig. 3). The calculated D_{Tc} value increases with an increase in DB18C6 concentration. For 0.1 M DB18C6 concentration in nitrobenzene, the removal of ^{99}Tc is about 89% ($D_{Tc} = 7.6$) in a single contact, which was found optimum. The extraction equilibrium for the TcO_4^- ions by the ligands can be expressed as

$$n{TcO_4}^-_{aq} + n{Na^+}_{aq} + nBD18C6_{NB} = [Na^+ \cdot BD18C6 \cdot TcO_4^-]_n \quad (2)$$

Following eqn (2), we can write,

$$K_{ex} = \frac{[Na^+ \cdot BD18C6 \cdot TcO_4^-]_n}{[TcO_4^-]^n_{aq}[Na^+]^n_{aq}\,[BD18C6]^n_{NB}} \quad (3)$$

Eqn (3) can be simplified further as,

$$K_{ex} = (D_{TcO_4^-})/([Na^+]^n_{aq}[BD18C6]^n_{NB} \quad (4a)$$

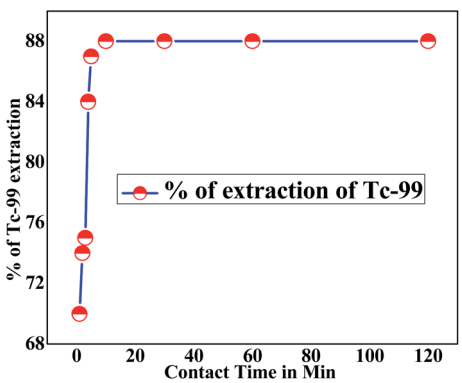

Fig. 2 Effect of equilibration time on the extraction of $^{99}TcO_4^-$. Organic phase: 0.1 M DB18C6 in nitrobenzene. Aqueous phase: LLW spiked with $^{99}TcO_4^-$ (triplicate measurements were done, and the error limit is ±5%).

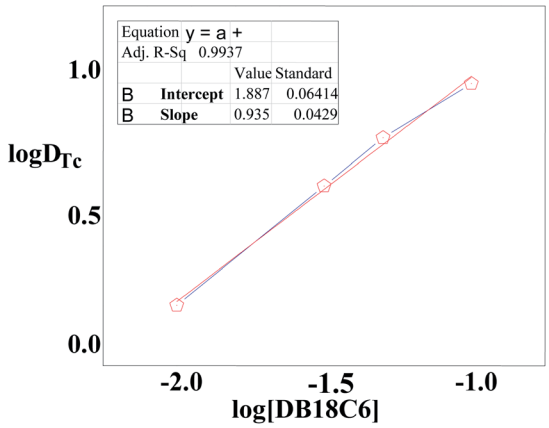

Fig. 3 Log D_{TC} *vs.* log[DB18C6] plot for the extraction of TcO_4^- as a function of DB18C6 concentration variation. Organic phase: different concentrations of DB18C6 in nitrobenzene. Aqueous phase: LLW spiked with $^{99}TcO_4^-$ (triplicate measurements were done, and the error limit is ±5%).

$$\log K_{ex} = \log D_{TcO_4^-} - n\log[Na^+]_{aq} - n\log[BD18C6]_{NB} \quad (4b)$$

$$\log D_{TcO_4^-} = \log K_{ex} + n\log[Na^+]_{aq} + n\log[BD18C6]_{NB} \quad (4c)$$

$$\log D_{TcO_4^-} = \log k'_{ex} + n\log[BD18C6]_{NB} \quad (4d)$$

$$k'_{ex} = \frac{D_{TcO_4^-}}{[BD18C6]_{NB}} \quad (4e)$$

While the Gibb's free energy change for the extraction equilibrium can be expressed as,

$$\Delta G = -2.303\ RT\log k'_{ex} \quad (5)$$

A plot of log D_{Tc} against log[BD18C6]$_{NB}$ (shown in Fig. 3) gave a straight line with a slope of 0.93, revealing the formation of a 1 : 1 metal–ligand complex. From the intercept, the conditional extraction constant and the change in Gibb's free energy have been evaluated as 79.43 mol^{-1} and −1.0708 kJ mol^{-1}, respectively, which are very close to the values reported from theoretical calculations.[41] The negative ΔG value for the extraction equilibrium suggests that the process is thermodynamically favourable and spontaneous.

3.3 Interference of nitrate and hydroxide ions on the extraction efficiency of ^{99}Tc

As the LLW contains a high concentration of $NaNO_3$ and NaOH, it is essential to know the interfering effects of NO_3^- and OH^- ions on the extraction efficiency for TcO_4^- ions by DB18C6 ligand. With this viewpoint, experiments were carried out for TcO_4^- ion extraction by 0.1 M DB18C6 in nitrobenzene in the presence of different concentrations (0.5–5.0) M of NaOH or $NaNO_3$ solution spiked with $^{99}TcO_4^-$ ions as a radiotracer in aqueous medium. Equilibrium time was kept for 20 min. Experimental results (Fig. 4a) revealed that up to about 3 M concentration of $NaNO_3$ or NaOH, the extraction efficiency

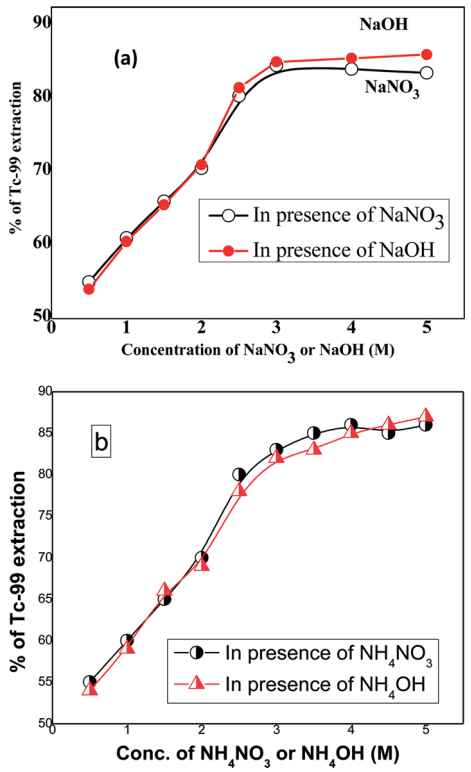

Fig. 4 Extraction profile for TcO_4^- ions by DB18C6 as a function of (a) $NaNO_3$ and NaOH; and (b) NH_4NO_3 and NH_4OH concentrations. Aqueous phase: different concentrations of NaOH or $NaNO_3$ (0.5–5.0) M, spiked with $^{99}TcO_4^-$ ions; organic phase: 0.1 M DB18C6 in nitrobenzene (triplicate measurements were done, and the error limit is ±5%).

increases steadily, and beyond this concentration, the extraction efficiency gets leveled off effectively. Beyond 3 M concentration, it is observed that the competitive effect of NO_3^- ions is somewhat stronger than OH^- ions, as the chemical behavior of NO_3^- ions is relatively closer to TcO_4^- ions as compared to the OH^- ions. Fig. 4b depicts a similar investigation using non-complexing counter ion like NH_4^+, and the results were found to be similar to that obtained by $NaNO_3$ and NaOH.

3.4 Determination of thermodynamic parameters

The temperature of the medium plays an important role in the extraction of metal ions using a ligand. Thus, temperature dependent measurements were also carried out to determine the extraction efficiency of TcO_4^- ions. So, experiments using organic phase 0.1 M DCH18C6 in nitrobenzene and aqueous phase spiked with $^{99}TcO_4^-$ ion radiotracer with varying temperatures were carried out. Experimental results reveal (Fig. 5) that with increasing temperature, the extraction of TcO_4^- ions by DB18C6 decreases substantially, indicating the overall extraction process to be largely exothermic in nature. These results may be explained in terms of the aqueous solubility of the metal–ligand complex. With the rise in temperature, the solubility of the complex increases substantially, and hence the organic phase contains a lesser amount of metal ions.

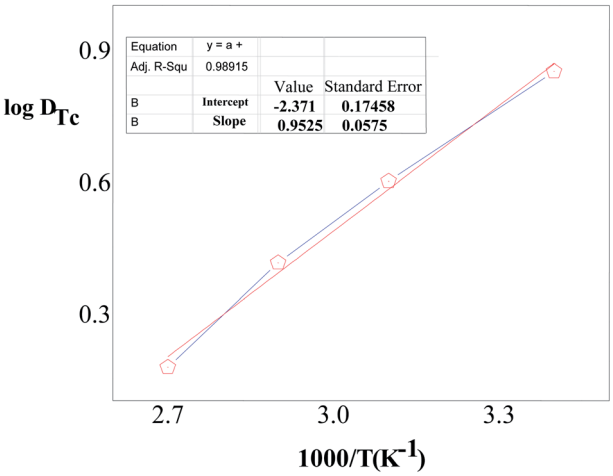

Fig. 5 The log D_{Tc} *vs.* $1/T$ plot for the extraction of TcO_4^- ions by DB18C6 ligand. Aqueous phase: spiked with $^{99}TcO_4^-$ ions; organic phase: 0.1 M DB18C6 in nitrobenzene (triplicate measurements were done and the error limit is ±5%).

The enthalpy change (ΔH) of the extraction equilibrium (6) can be evaluated using the Van't Hoff equation as,

$$\Delta H = -2.303R\Delta \log D/\Delta(1/T) \quad (6)$$

From eqn (6), the plot of log D *vs.* $1/T$ would give a straight line with a slope as $\Delta H/2.303R$. Further, the Gibb's free energy change (ΔG) for the process can be evaluated from eqn (7).

$$\Delta G = -2.303RT \log K_{Tc} \quad (7)$$

Subsequently, the change in entropy (ΔS) can be determined at a particular temperature using eqn (8).

$$\Delta G = \Delta H - T\Delta S \quad (8)$$

From the slope of the log D *vs.* $1/T$ plot, the ΔH value for the extraction equilibrium (6) is found to be about −18.2 kJ mol^{-1}. Accordingly, following eqn (6) and (7), the ΔG and ΔS values for the overall extraction process are estimated to be about −1.07 kJ mol^{-1} and −57.48 J mol^{-1}, respectively. The largely negative ΔS value can be attributed to the reduction in the number of free ions in the reaction medium during complex formation.

3.5 Effect of solution pH on extraction efficiency of TcO_4^-

As pH of the solution greatly affects the extraction of metal ions as the Tc chemistry is very complex in nature, and the speciation of Tc depends significantly across the pH range. Yalçıntaş, E. *et al.*[55] reported the redox nature of Tc(VII)/Tc(IV) within pH range from 2 to 14.6 in solutions of (0.5 M and 5.0 M) NaCl and (0.25 M, 2.0 M, and 4.5 M) $MgCl_2$ in the presence of reducing agents like Sn(II), $Na_2S_2O_4$, Fe(II)/Fe(III), and Fe powder. These experimental observations revealed that pH and E_h values in a buffered medium could be considered as potential parameters

to predict the redox nature of Tc in dilute solutions to concentrated $MgCl_2$ and NaCl solutions. The E_h value of the system and also an aqueous concentration of Tc(IV) with $TcO_2 \cdot 1.6H_2O$(s) in equilibrium are significantly affected by high ionic strength, particularly in the case of 4.5 M $MgCl_2$ solutions. In the presence of concentrated brines and alkaline conditions (pH = pH_{max} 9) Tc(VII) is reduced to Tc(IV) using magnetite, mackinawite[56] at pH = 8–9 in the presence of concentrated $MgCl_2$ and NaCl solutions. Here, we have obtained the extraction profile of TcO_4^- ions at different pH values of the medium (pH 1–14) (Fig. 6), maintaining the ionic strength in solution in the aqueous phase. The extraction profile of ^{99}Tc increases from pH 1 to 3 and subsequently decreases till up to neutral pH. Subsequently, the extraction efficiency starts to increase again in the alkaline region and reaches a kind of saturation from pH 12 onward. These results can be explained in terms of the binding selectivity of DB18C6 towards alkali metal (Na^+) ions that determines the stability of the Na^+–DB18C6·TcO_4^- complex. In an aqueous solution, the solvation energy of Na^+–DB18C6 plays a vital role in the binding selectivity of DB18C6 for Na^+.[41] The interaction *via* non-electrostatic dispersion between the solvent and solute, which also depends on the complex structure as well as accountable for the solvation energies of Na^+–DB18C6, which in turn contributes to the stability of the Na^+–DB18C6·TcO_4^- complex. Solvation energy of Na^+–DB18C6 has a significant role in relative bond dissociation free energies (BDFE) of Na^+–DB18C6 followed by the binding selectivity of DB18C6 towards Na^+ ions in aqueous solution. So, the non-electrostatic and electrostatic dispersion interactions between the solvent and solute play a vital role, which also influences the stability of the Na^+–DB18C6 complex along with a large contribution for solvation energies of the Na^+–DB18C6 complex. Therefore, these interactions, which strongly control the solvation energy, are followed by the stability and binding selectivity of complex formation. At neutral pH, where charge species in the solution are less, the electrostatic dispersion interaction does not operate that strongly, resulting in lowering the binding selectivity of DB18C6 for Na^+ ions and thereby reducing the Na^+–DB18C6·TcO_4^- complex formation effectively. On the other hand, at the acidic and alkaline pH conditions, where the charge species are abundant, the electrostatic dispersion interaction operates very strongly, leading to the strong binding selectivity of DB18C6 towards Na^+ ions and consequently enhancing the stability of the Na^+–DB18C6·TcO_4^- complex, giving higher extraction efficiency in effect.

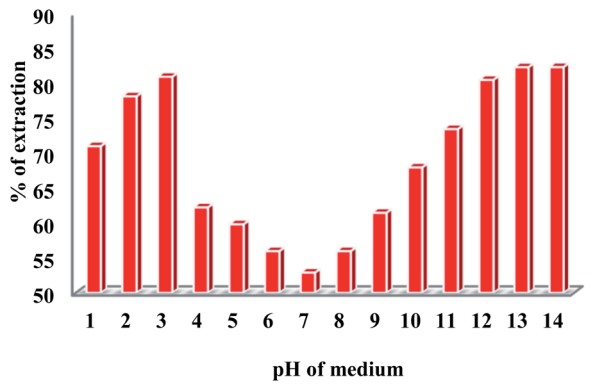

Fig. 6 Effect of solution pH on the extraction efficiency of TcO_4^- by DB18C6. Aqueous phase: solution at different pH (1–14) values spiked with $^{99}TcO_4^-$ radiotracer; organic phase: 0.1 M DB18C6 in nitrobenzene (triplicate measurements were done and the error limit is ±5%).

3.6 Stripping study

For waste management, for the reuse of the DB18C6 ligand, a stripping study is very much required. Hence, in the present work stripping studies were carried out using water and nitric acid solution as the stripping agents. Stripping of ^{99}Tc was increased with the increase in acidity of the stripping solution, as shown in Fig. 7. Using water as a stripping agent, only 5% Tc was found to be back extracted from the loaded organic phase, while using 0.1 M HNO_3 and 0.01 M HNO_3, the % stripping was found to be within 20–25%. However, a sharp enhancement with maximum stripping of ~77% was observed when 1 M HNO_3 was used as a stripping agent.

3.7 Selectivity and feasibility study of TcO_4^- extraction process

After evaluating all necessary parameters for the extraction of TcO_4^- ions by DB18C6, experiments were carried out to evaluate the feasibility as well as selectivity of the present process for extraction of TcO_4^- ions from reprocessing alkaline (pH = 13) plant LLW sample using 0.1 M DB18C6 in nitrobenzene as the extractant. Experimental result reveals that about 90% of ^{99}Tc activity is trapped in the DB18C6/organic phase. As the results in Table 2 indicate, the separation of ^{99}Tc is much higher as compared to ^{137}Cs and ^{90}Sr. This is due to the binding selectivity of DB18C6 in the nitrobenzene solvent system towards alkali metal ions, which is strongly dependent on the size of the metal ions as well as their hydration energy.

3.8 Proposed TcO_4^- extraction and stripping mechanism

The extraction and stripping mechanism of TcO_4^- ions by DB18C6 can be explained by the size selective reversible complex formation between alkali metal Na^+ ions and DB18C6, as the cavity size of DB18C6 matches with Na^+ radius.[41] This

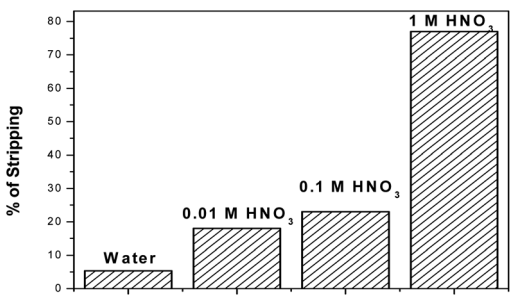

Fig. 7 Stripping of TcO_4^- using water and different concentrations of nitric acid solution as the stripping agent.

Table 2 Extraction of TcO_4^- and other (^{137}Cs and ^{90}Sr) fission products from actual LLW samples. Organic phase: 0.1 M DB18C6 in nitrobenzene. Aqueous phase: LLW. Organic : aqueous = 1 : 1 (triplicate measurements were done, and the error limit is ±5%)

S. No.	Species	Before extraction (activity mCi L^{-1})	After extraction (activity mCi L^{-1})	D_M	S. F. (D_{Tc}/D_M)
1	Gross β	0.45	0.047	8.6	—
2	Tc-99	0.30	0.035	7.6	—
3	Sr-90	5×10^{-4}	2.5×10^{-4}	1	7.6
4	Cs-137	5×10^{-3}	1.5×10^{-3}	2.3	3.3

$[DB18C6 \cdot Na^+]$ complexes subsequently bind the TcO_4^- ions to form $[DB18C6 \cdot Na^+ \cdot TcO_4^-]$ complexes, as shown schematically in Fig. 8 and eqn (9). The LLW samples from the reprocessing spent fuel contain a very high concentration of Na^+ ions. Thus, these Na^+ ions derive the overall reaction favorably towards the formation of $[DB18C6 \cdot Na^+ \cdot TcO_4^-]$ complexes participating in the extraction process. In the extraction process, the formation of size selective stable complexes between Na^+ and DB18C6 enhances the extraction process over the conventional salting out effect at high salt concentrations. In the present process, since DB18C6 is a neutral ligand and Na^+ is a unipositive cation, the resultant $[DB18C6 \cdot Na^+]$ complex possesses a unit positive charge. Accordingly, for the enhancement of the stability, the so formed $DB18C6 \cdot Na^+$ complex requires to be associated with an anion, in this the TcO_4^- ion, to achieve the charge neutralization for the overall $[DB18C6 \cdot Na^+ \cdot TcO_4^-]$ complex, which is effectively extracted in the organic phase. From Fig. 5 it is clear that DB18C6 is directly participating in the mass transfer of Tc. Tc exists as TcO_4^- ion in the acidic feed under consideration. It was also evidenced from this slope ratio method that one DB18C6 ligand was attached with one Tc species. Therefore, the expected species would be $TcO_4^-[DB18C6]$. Since the overall charge of the complex was unit negative, so to maintain electrical neutrality, the unit positive charge cation must be associated with it during the effective mass transfer of Tc. As reported earlier, Na^+ had a tendency to sit in the cavity of DB18C6 due to size selectivity. Therefore, in the presence of Na^+, most likely, $Na[DB18C6]TcO_4$ could be the species involved in mass transfer. The argument is quite logical and can be accepted. Stripping is accomplished by simply reversing this complexation equilibrium. The organic phase containing the $[DB18C6 \cdot Na^+ \cdot TcO_4^-]$ complex is contacted with deionized water and acid, promoting the dissociation of the complex whereby the free Na^+ and TcO_4^- ions are partitioned into the aqueous phase, and the free crown ether remains in the organic phase. Eqn (9) represents the extraction reaction.

$$Na^+ + TcO_4^- + DB18C6 = [DB18C6 \cdot Na^+ \cdot TcO_4^-] \quad (9)$$

3.9 Structure and structural parameters

The optimized structures of DB18C6, $DB18C6–Na^+$, DB18C6–Na–TcO_4, DB18C6–Na–TcO_4^- $(NB)_3$ (NB – nitrobenzene), DB18C6–Na–TcO_4^- $(CB)_4$ (CB – chlorobenzene), and DB18C6–Na–$TcO_4^-(TCE)_4$ (TCE – trichloroethylene) at B3LYP/TZVP level of theory are displayed in Fig. 9, and structural parameters are given in Table 3. In the case of all the studied complexes, Na^+ ion is encapsulated in the cavity of DB18C6, and O atom(s) of TcO_4^- is coordinated to Na^+ ion, which is in the cavity of DB18C6. In the case of DB18C6–Na–TcO_4, the average Na–O(DB18C6), Na–O(TcO_4^-), and Tc–O bond distances were found to be 2.725, 2.899, and 1.732 Å, respectively. To study the effect of solvents, NB, CB, and TCE are explicitly solvated on the DB18C6–Na–TcO_4^- complex. Initially, the [DB18C6–Na–TcO_4] complex is solvated with 4 solvent molecules. However,

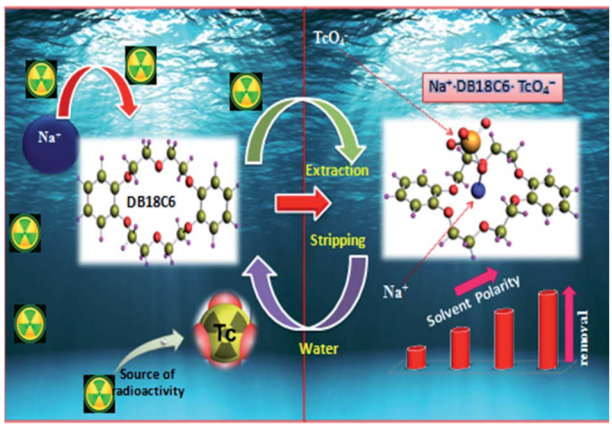

Fig. 8 Mechanism of TcO_4^- extraction by crown ether from a waste stream containing alkali metal ions and stripping with water/acid.

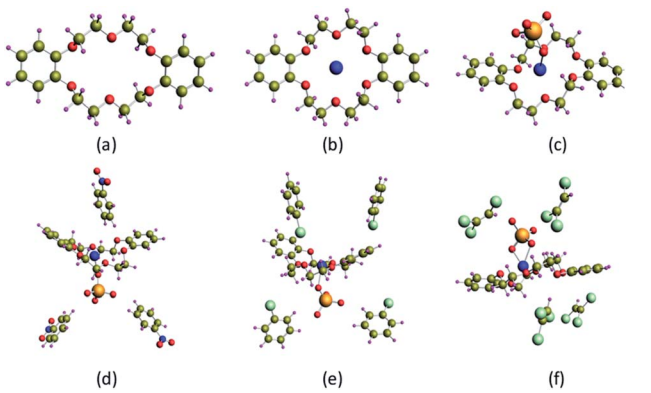

Fig. 9 Optimized structures of (a) DB18C6, (b) $DB18C6–Na^+$, (c) DB18C6–Na–TcO_4, (d) DB18C6–Na–TcO_4–$(NB)_3$, (e) DB18C6–Na–TcO_4–$(CB)_4$, and (f) DB18C6–Na–TcO_4–$(TCE)_4$ at B3LYP/TZVP level of theory.

Table 3 Structural parameters of "Tc" complexes with DB18C6 at B3LYP/TZVP level of theory

Species	Average Na–O(DB18C6), Å	Average Na–O(TcO_4^-), Å	Tc–O, Å
DB18C6–Na–TcO_4	2.725	2.899	1.732
DB18C6–Na–TcO_4–$(NB)_3$	2.588	3.103	1.731
DB18C6–Na–TcO_4–$(CB)_4$	2.682	3.293	1.731
DB18C6–Na–TcO_4–$(TCE)_4$	2.899	2.564	1.732

DB18C6–Na–TcO_4–$(NB)_4$ failed to get optimized and led to DB18C6–Na–$TcO_4^-$$(NB)_3$ with 1 NB molecule far apart from the complex. Hence, we have considered DB18C6–Na–TcO_4^- $(NB)_3$ complex for further study. In the case of DB18C6–Na–TcO_4–$(NB)_3$ and DB18C6–Na–TcO_4–$(CB)_4$ complexes, the average Na–O(DB18C6) distances were found to be decreased, and Na–O(TcO_4^-) distances were found to be increased compared to DB18C6–Na–TcO_4 complex. Whereas, Tc–O distances were found to be unaffected. In the case of DB18C6–Na–$TcO_4^-$$(TCE)_4$ complex, Na–O(DB18C6) distances were found to be increased, and Na–O(TcO_4^-) distances were found to be decreased compared to the DB18C6–Na–TcO_4 complex. The Na–O(TcO_4^-) bond distance in the CB solvent is found to be longer compared to the NB solvent and may be the reason for more stability of the DB18C6–Na–TcO_4 complex in the NB solvent compared to CB solvent. Whereas in the case of TCE solvent, correlation cannot be drawn as the Na–O(DB18C6) distance was found to increase compared to its gas phase DB18C6–Na–TcO_4 complex.

3.10 Binding energy/free energy of complexation

From the experimental observations, the metal ion-ligand complexation reaction is modeled as the 1 : 1 (M : L) stoichiometric reaction as follows:

Gas phase

$$TcO_4^-(g) + Na^+(g) + DB18C6(g) \rightarrow DB18C6\text{–}Na\text{–}TcO_4(g) \quad (10)$$

Solvent phase

$$TcO_4^-(aq) + Na^+(aq) + DB18C6(org) \rightarrow DB18C6\text{–}Na\text{–}TcO_4(org) \quad (11)$$

The selectivity for a particular metal ion towards a complexion ligand can be explained using binding energy or free energy. Hence, the gas phase binding energy is computed for the complexation reaction of eqn (10) as follows.

$$\Delta E = E_{DB18C6\text{–}Na\text{–}TcO_4^-} [E_{TcO_4^-} + E_{Na^+} + E_{DB18C6}] \quad (12)$$

The thermal correction to the electronic energy (E_{el}), enthalpy (H), and free energy (G) of the optimized complexes has been performed following the earlier reported prescription.[1,57,58] The calculated values of B.E., ΔE, and free energy of complexation ΔG in the gas and solvent phases using implicit solvation model are presented in Table 4 (equation (A)). Equation (A) represents treating "Na" as a bare metal ion without solvation. From the calculated values of ΔE and ΔG in the gas phase, it is observed that ΔG value is found to be lower than ΔE, which is due to the complex formation process. Further, from the calculated values of ΔE in the solvent phase, it is observed that the complexation of TcO_4^- follows the order NB > CB > TCE, which is not in line with experimental results (see Section 3.11, Table 6) and the calculated ΔG values were found to be positive.

To retrieve the experimental selectivity, the above complexation reaction is modelled by including the Na^+–$(H_2O)_6$ cluster instead of Na^+ ion, which is strongly hydrated compared to TcO_4^- in the calculations (equation (B)). In equation (B), the Na^+ ion is replaced by Na^+–$(H_2O)_6$ cluster in eqn (10) and (11). Now the complexation reaction can be modelled as

$$TcO_4^-(g) + Na^+\text{–}(H_2O)_6(g) + DB18C6(g) \rightarrow DB18C6\text{–}Na\text{–}TcO_4(g) + 6H_2O \quad (13)$$

$$TcO_4^-(aq) + Na^+\text{–}(H_2O)_6(aq) + DB18C6(org) \rightarrow DB18C6\text{–}Na\text{–}TcO_4(org) + 6H_2O \quad (14)$$

The calculated values of B.E., ΔE, and free energy of complexation ΔG in the gas and solvent phases using Na^+–$(H_2O)_6$ (equation (B)) cluster are presented in Table 2. From the calculated values of ΔE and ΔG in the gas phase, it is observed that ΔG value is found to be higher than ΔE, which is due to the release of water molecules in the complexation process. The calculated ΔE values were found to be positive and ΔG values were found to be negative, which is the reverse of earlier observation with equation (A). Further, from the calculated

Table 4 Gas and solvent phase energetic values (kcal mol^{-1}) of complexes of TcO_4^- with DB18C6 at B3LYP/TZVP level of theory using an implicit model. A and B represent Na^+ or Na–$(H_2O)_6$, respectively

	Gas phase (A)		Gas phase (B)	
Complex	ΔE	ΔG	ΔE	ΔG
DB18C6–Na–TcO_4	−158.26	−135.70	−47.60	−90.75
	Solvent Phase		Solvent Phase	
Complex	ΔE	ΔG	ΔE	ΔG
DB18C6–Na–TcO_4 in nitrobenzene	−15.22	7.35	13.98	−29.17
DB18C6–Na–TcO_4 in chlorobenzene	−14.04	8.52	15.15	−28.00
DB18C6–Na–TcO_4 in trichloroethylene	−13.17	9.39	16.02	−27.13

Table 5 Gas and Solvent phase energetic values (kcal mol^{-1}) of complexes of TcO_4^- with DB18C6 at B3LYP/TZVP level of theory using an explicit model. A and B represent Na^+ or $Na–(H_2O)_6$, respectively

	Gas phase (A)		Gas phase(B)	
Complex	ΔE	ΔG	ΔE	ΔG
DB18C6–Na–TcO_4–$(NB)_3$	−166.49	38.35	−55.82	−7.40
DB18C6–Na–TcO_4–$(CB)_4$	−169.72	35.20	−59.05	−10.56
DB18C6–Na–TcO_4–$(TCE)_4$	−163.56	31.57	−52.90	−14.19
	Solvent Phase		Solvent Phase	
Complex	ΔE	ΔG	ΔE	ΔG
DB18C6–Na–TcO_4–$(NB)_3$ in nitrobenzene	−16.88	18.79	12.32	−17.73
DB18C6–Na–TcO_4–$(CB)_4$ in chlorobenzene	−19.46	21.36	9.73	−15.16
DB18C6–Na–TcO_4–$(TCE)_4$ in trichloroethylene	−13.32	20.84	15.87	−15.68

values of ΔG in the solvent phase, it is observed that the complexation of TcO_4^- follows the order NB > CB > TCE, which is not in line with experimental results (see Section 3.11, Table 6). So, consideration of the $Na^+–(H_2O)_6$ cluster was also not able to predict the experimental selectivity.

In the next step, the DB18C6–Na–TcO_4 complex is explicitly solvated with NB, CB, and TCE solvent molecules to explain the experimental selectivity of TcO_4^- with DB18C6. The complexation reactions with explicit solvent molecules in the complex using equation (A) and (B) can be modelled as.

Gas phase

$$TcO_4^-(g) + Na^+(g) + DB18C6(g) + (S)_m \rightarrow DB18C6–Na–TcO_4–(S)_m(g) \quad (15)$$

(where, S = NB, CB or TCE, m = 3–4).

Solvent phase

$$TcO_4^-(g) + Na^+(aq) + DB18C6(org) + (S)_m org \rightarrow DB18C6–Na–TcO_4–(S)_m(org) \quad (16)$$

Gas phase

$$TcO_4^-(g) + Na^+–(H_2O)_6(g) + DB18C6(g) + (S)_m(g) \rightarrow DB18C6–Na–TcO_4–(S)_m(g) + 6H_2O \quad (17)$$

Solvent phase

$$TcO_4^-(g) + Na^+–(H_2O)_6(aq) + DB18C6(org) + (S)_m org \rightarrow DB18C6–Na–TcO_4–(S)_m(org) + 6H_2O \quad (18)$$

The calculated values of ΔE and ΔG of TcO_4^- in the gas and solvent phases using Na^+ (equation (A)) and $Na^+–(H_2O)_6$ (equation (B)) cluster with explicit solvents in the complex are presented in Table 5. From the calculated ΔE values with equation (A) and equation (B) in the gas phase, it is observed that the complexation of TcO_4^- follows the order CB > NB > TCE, which is not in line with the experimental results (see Section 3.11, Table 6). Further, it is observed that in the solvent calculations, ΔE values using equation (A) follows a similar order as that of ΔE values in the gas phase. So, the experimental trend was recovered using eqn (15)–(17).

The experimental trend was recovered in the ΔG values in the solvent phase using equation (B) (eqn (18)). The calculated values of ΔG for TcO_4^- in the solvent phase with explicit solvent molecules in the DB18C6–Na–TcO_4 complex are −17.73, −15.68, and −15.16 kcal mol^{-1} in the NB, TCE, and CB solvents, which follows the order NB > TCE > CB, as observed in the experimental results (see Section 3.11, Table 6). Hence, we found the importance of explicit solvent molecules in complexation in the present study. Further, the studies can be extended with the incorporation TcO_4^- hydration and variation of solvent molecules in the complex, which is beyond the scope of the present study.

3.11 Comparative evaluation of TcO_4^- extraction

Table 6 summarizes the experimental results for TcO_4^- extraction by the two most promising crown ether based ligands in different solvent systems that are reported in the literature to compare the present experimental results from the earlier studies reported. It is established that the formation of a 1 : 1 metal–ligand complex as well as the size selectivity are the key driving forces for the mass transfer of the target metal ions (TcO_4^-) to the organic phase from an aqueous medium. The maximum D_{Tc} value achieved in the present case is found to be considerably higher with respect to all the solvent systems

Table 6 A comparative study on $^{99}TcO_4^-$ extraction by crown ether in different diluents

Ligand	Solvent	Dielectric constant	Metal : ligand ratio	D_{Tc}	Ref.
DB18C6	Nitrobenzene	34.82	1 : 1	7.6	Present study
Di-*t*-BuDB18C6	Isodecyl alcohol/*n*-dodecane	—	1 : 1	4.46	39
DB18C6	Benzene	2.275	1 : 1	0.0016	42
DB18C6	Trichloroethylene	3.42	1 : 1	0.011	
DB18C6	1,2,4-Trichlorobenzene	—	1 : 1	0.0037	
DB18C6	Chloroform	4.806	1 : 1	0.0076	
DB18C6	Chlorobenzene	5.621	1 : 1	0.0028	
DB18C6	*o*-Dichlorobenzene	9.93	1 : 1	0.033	
DB18C6	1,2-Dichloroethane	10.36	1 : 1	0.155	

reported, as indicated clearly in Table 6. Among the other literature reports, the result reported by Sharma *et al.* using di-*t*-BuDB18C6 in isodecyl alcohol/*n*-dodecane solvent shows a significantly higher D_{Tc} value,[39] but this value is still much lower than that estimated in the present study. Comparing the effects of the diluents on ^{99}Tc extraction using DB18C6 and di-*t*-BuDB18C6 ligands reveal that the extraction efficiency follows the order:

Nitrobenzene > isodecyl alcohol/*n*-dodecane > 1,2-dichloromethane > *o*-dichlorobenzene > trichloroethylene > chloroform > chlorobenzene > 1,2,4-trichlorobenzene > benzene. This comparative evaluation definitely indicates that DB18C6 in nitrobenzene (present case) is the most efficient system for the extraction of $^{99}TcO_4^-$ from LLW samples.

4. Conclusion

In summary, we herein present the study on $^{99}TcO_4^-$ separation using DB18C6 ligand in a highly polar nitrobenzene solvent system, showing promising results for the extraction of TcO_4^- ions ($D_{TC} = 7.6$, around 88% removal) from aqueous alkaline waste. From the experimental results, it is inferred that the extraction of $^{99}TcO_4^-$ can be considerably enhanced using DB18C6 as an extractant in the presence of a highly polar solvent, nitrobenzene. The high selectivity of $^{99}TcO_4^-$ separation is mainly due to the strong binding selectivity of DB18C6 towards Na^+ ions resulting in high stability of the resultant DB18C6·Na^+·TcO_4^- complex, where TcO_4^- plays the role of a charge neutralizing agent for the initially formed cationic DB18C6·Na^+complex. The effect of relevant anions present in the waste, like the nitrate and hydroxide ions, on the extraction behaviour of ^{99}Tc has also been evaluated. The optimum contact time for maximum extraction is around 20 min. The effect of pH on the extraction process has also been carried out systematically. Thermodynamic parameters of the extraction equilibrium have been estimated from temperature dependent extraction studies. It is found that with the rise in temperature, the extraction efficiency of TcO_4^- ions by DB18C6 decreases substantially. DFT calculations were carried out to understand the complexation of TcO_4^- ion with DB18C6 in different solvents. The ΔE and ΔG values for different modelled complexation reactions were evaluated. From the calculated free energy of complexation of TcO_4^- with DB18C6, it is observed that the consideration of an explicit solvent play a very important role for predicting the experimental selectivity. The analytical implication of this research work lies with the much higher estimate of the distribution ratio (D_{Tc}) as compared to the literature reports, and this methodology can be used for the selective extraction of ^{99}Tc from LLW, which is of major importance to minimize the hazardous effect of TcO_4^- in LLW, to avoid the long term radiological surveillance.

Conflicts of interest

There are no conflicts to declare.

Acknowledgements

We acknowledge Dr H. Pal, former AD, Chemistry Group, BARC, Dr C. P. Kaushik AD, NRG, BARC, Dr R. K Mishra, SO/F, NRG, BARC and Dr Biswajit Sadhu, SO/E HPD, NRG, BARC for his constant encouragement. We also would like to acknowledge U. Dani, GM, INRPO (R & WM), BARC and Sanjay Pradhan, Dy. CE, NRB, BARC. The author also wish to acknowledge Dr P. K. Pujari, Director, RC & I Group, Head, Radiochemistry Division, BARC and Dr R. Acharya, Head, Spectroscopy Section, Radiochemistry Division, BARC.

References

1 M. S. Dresselhaus and I. L. Thomas, *Nature*, 2001, **414**, 332–337.
2 M. Singh, A. Sengupta, M. S. Murali and R. M. Kadam, *J. Radioanal. Nucl. Chem.*, 2016, **309**, 1199–1208.
3 C. W. Abney, R. T. Mayes, T. Saito and S. Dai, *Chem. Rev.*, 2017, **117**, 13935–14013.
4 M. Singh, A. Sengupta, M. S. Murali and R. M. Kadam, *J. Radioanal. Nucl. Chem.*, 2016, **309**, 615–625.
5 Y. Yuan, Y. Yang, X. Ma, Q. Meng, L. Wang, S. Zhao and G. Zhu, *Adv. Mater.*, 2017, **30**, 1706507.
6 A. Sengupta, M. S. Murali, S. K. Thulasidas and P. K. Mohapatra, *Hydromet*, 2014, **147–148**, 228–233.
7 A. Sengupta, P. K. Mohapatra, M. Iqbal, J. Huskens and W. Verboom, *Supramol. Chem.*, 2014, **26**(7–8), 612–619.
8 A. Sengupta, P. K. Mohapatra, R. M. Kadam, D. Manna, T. K. Ghanty, M. Iqbal, J. Huskens and W. Verboom, *RSC Adv.*, 2014, **4**, 46613–46623.
9 J. G. Darab and P. A. Smith, *Chem. Mater.*, 1996, **8**, 1004–1021.
10 J. P. Icenhower, N. P. Qafoku, J. M. Zachara and W. J Martin, *Am. J. Sci.*, 2010, **310**(8), 721–752.
11 R. Alberto, G. Bergamaschi, H. Braband, T. Fox and V. Amendola, *Angew. Chem., Int. Ed.*, 2012, **51**, 9772–9776.
12 K. Ito and A. Yachidate, *Carbon*, 1992, **30**, 767–771.
13 B. Gu and K. E. Dowlen, *An Investigation of Groundwater Organics, Soil Minerals, and Activated Carbon on the Complexation, Adsorption, and Separation of Technetium-99, Publication No. 4502*, Environmental Sciences Division, ORNL/TM-13154, Oak Ridge, Tennessee, 1996.
14 S. V. Mattigod, R. J. Serne and G. E. Fryxell, *Selection and Testing of "Getters" for Adsorption of Iodine-129 and Technetium-99: A Review, PNNL-14208*, 2003.
15 D. Banerjee, D. Kim, M. J. Schweiger, A. A. Kruger and P. K. Thallapally, *Chem. Soc. Rev.*, 2016, **45**, 2724–2739.
16 J. P. Icenhower, N. P. Qafoku, J. M. Zachara and W. J. Martin, *Am. J. Sci.*, 2010, **310**, 721–752.
17 R. Carmody and J. H. Highman, *Br. J. Radiol.*, 1975, **48**, 63–64.
18 K. Raj, K. K. Prasad and N. K. Bansal, *Nucl. Eng. Des.*, 2006, **236**, 914–930.
19 M. L. Kathryn, T. Pashow, D. J. McCabe and C. A. Nash, *Sep. Sci. Technol.*, 2017, **53**, 1925–1934.

20 P. V Bonnesen, G. M. Brown and L. B. Bavoux, *Environ. Sci. Technol.*, 2000, **34**, 3761–3766.
21 K. K. S. Pillay, *J. Radioanal. Nucl. Chem.*, 1986, **102**, 247–268.
22 J. Li, L. Zhu, C. Xiao, L. Chen, Z. Chai and S. Wang, *Radiochim. Acta*, 2018, **106**, 581–591.
23 F. Gándara, J. Perles, N. Snejko, M. Iglesias, B. Gómez-Lor, E. Gutiérrez-Puebla and M. Angeles Monge, *Angew. Chem., Int. Ed.*, 2016, **45**, 7998–8001.
24 Y. Wang and H. Gao, *J. Colloid Interface Sci.*, 2006, **301**, 19–26.
25 L. Zhu, L. Zhang, J. Li, D. Zhang, L. Chen, D. Sheng, S. Yang, C. Xiao, J. Wang, Z. Chai, T. E. Albrecht-Schmitt and S. Wang, *Environ. Sci. Technol.*, 2017, **51**, 8606–8615.
26 S. Wang, E. V. Alekseev, J. Diwu, W. H. Casey, B. L. Phillips, W. Depmeier and T. E. Albrecht-Schmitt, *Angew. Chem., Int. Ed.*, 2010, **49**, 1057–1060.
27 S. Wang, P. Yu, B. A. Purse, M. J. Orta, J. Diwu, W. H. Casey, B. L. Phillips, E. V. Alekseev, W. Depmeier, D. T. Hobbs and T. E. Albrecht-Schmitt, *Adv. Funct. Mater.*, 2012, **22**, 2241–2250.
28 D. Sheng, L. Zhu, C. Xu, C. Xiao, Y. Wang, Y. Wang, L. Chen, J. Diwu, J. Chen, Z. Chai, T. E. Albrecht-Schmitt and S. Wang, *Environ. Sci. Technol.*, 2017, **51**, 3471–3479.
29 L. Zhu, C. Xiao, X. Dai, J. Li, D. Gui, D. Sheng, L. Chen, R. Zhou, Z. Chai, T. E. Albrecht-Schmitt and S. Wang, *Environ. Sci. Technol. Lett.*, 2017, **4**, 316–322.
30 L. Zhu, D. Sheng, C. Xu, X. Dai, M. A. Silver, J. Li, P. Li, Y. Wang, Y. Wang, L. Chen, C. Xiao, J. Chen, R. Zhou, C. Zhang, O. K. Farha, Z. Chai, T. E. Albrecht-Schmitt and S. Wang, *J. Am. Chem. Soc.*, 2017, **139**, 14873–14876.
31 D. Banerjee, W. Xu, Z. Nie, L. E. V. Johnson, C. Coghlan, M. L. Sushko, D. Kim, M. J. Schweiger, A. A. Kruger, C. J. Doonan and P. K. Thallapally, *Inorg. Chem.*, 2016, **55**, 8241–8243.
32 M. Y. Suh, C. H. Lee, S. H. Han, J. S. Kim, Y. J. Park and W. H. Kim, *Korean Chem. Soc.*, 2003, **24**(11), 1686–1688.
33 C. Nash, B. Musall, M. Morse and D. McCabe, *Sep. Sci. Technol.*, 2015, **50**, 2881–2887.
34 B. R. Harvey, K. J. Williams, M. B. Lovett and R. D. Ibbett, *J. Radioanal. Nucl. Chem.*, 1992, **158**(2), 417–436.
35 V. De, N. L. Sonar, Y. Raghavendra, T. P. Valsala, M. S. Sonavane, S. Jain, Y. Kulkarni and R. D. Changrani, *Desalin. Water Treat.*, 2012, **38**, 22–28.
36 E. H. Huffman, R. L. Oswalt and L. A. Williams, *J. Inorg. Nucl. Chem.*, 1956, **3**, 49–53.
37 M. Pirs and R. J. Magee, *Talanta*, 1961, **8**, 395–399.
38 P. V. Bonnesen, B. A. Moyer, D. J. Presley, V. S. Armstrong, T. J. Haverlock, R. M. Counce and R. A. Sachleben, *Alkaline-Side Extraction of Technetium from Tank Waste Using Crown Ethers and Other Extractants*, ORNL/TM-13241 Chemical and Analytical Sciences Division, 1996.
39 J. N. Sharma, P. Sinharoy, B. Kharwandikar, V. S. Thorat, V. Tessy and C. P. Kaushik, *Sep. Purif. Technol.*, 2018, **207**, 416–419.
40 W. Derec, *J. Chem. Educ.*, 1977, **54**(9), 540–542.
41 C. Min Choi, J. Heo and N. J. Kim, *Chem. Cent. J.*, 2012, **6**, 84.
42 M. G. Jalhoom, *Radiochim. Acta*, 1986, **39**, 195–197.
43 N. L. Sonar, V. De, V. Pardeshi, Y. Raghavendra, T. P. Valsala, M. S. Sonavane, Y. Kulkarni and R. Kanwar, *J. Radioanal. Nucl. Chem.*, 2012, **294**, 185–189.
44 A. D. Becke, *J. Chem. Phys.*, 1993, **98**(2), 1372–1377.
45 C. Lee, W. Yang and R. G. Parr, *Phys. Rev. B*, 1988, **37**(2), 785.
46 TurbomoleV7.2, A development of University of Karlsruhe and Forschungszentrum Karlsruhe GmbH (1989–2007) TURBOMOLE GmbH, since (2007). 2009.
47 A. Klamt, *J. Phys. Chem.*, 1995, **99**(7), 2224–2235.
48 A. Klamt and G. Schuurmann, *J. Chem. Soc., Perkin Trans.*, 1993, **2**(5), 799–805.
49 G. Salunkhe, A. Sengupta, A. Boda, R. Paz, N. K. Gupta, C. Leyva, R. S. Chauhan and Sk. M. Ali, *Chemosphere*, 2022, **287**, 132232.
50 A. Boda and M. A. Sheikh, *J. Phys. Chem. A*, 2012, **116**(33), 8615–8623.
51 A. Boda, A. K. S. Deb, A. Sengupta, Sk. M. Ali and K. T. Shenoy, *Polyhedron*, 2017, **123**, 234–242.
52 S. Pathak, Sk. Jayabun, A. Boda, S. K. M Ali and A. Sengupta, *J. Mol. Liq.*, 2020, **316**, 113864.
53 N. K. Gupta, A. Sengupta, A. Boda, V. C. Adya and S. M. Ali, *RSC Adv.*, 2016, **6**(82), 78692–78701.
54 A. Sengupta, S. Jayabun, A. Boda and S. M. Ali, *RSC Adv.*, 2016, **6**(46), 39553–39562.
55 E. Yalçıntaş, X. Gaona, A. C. Scheinost, T. Kobayashi, M. Altmaier and H. Geckeis, *Radiochim. Acta*, 2015, **103**(1), 57–72.
56 E. Yalçıntaş, A. C. Scheinost, X. Gaonaa and M. Altmaiera, *Dalton Trans.*, 2016, **45**, 17874–17885.
57 M. Adrian-Scotto, G. Mallet and D. Vasilescu, *J. Mol. Struct.: THEOCHEM*, 2005, **728**(1), 231–242.
58 J. P. Perdew, K. Burke and M. Ernzerhof, *Phys. Rev. Lett.*, 1996, **77**(18), 3865–3868.